

# *Analysis of Shoulder Impingement and Stability in Tennis Players*

Charbonnier C. <sup>1</sup>, Chagué S. <sup>1</sup>, Kolo F.C. <sup>2</sup>, Lädermann A. <sup>3,4</sup>

<sup>1</sup> Artanim Foundation, Medical Research Department, Geneva, Switzerland

<sup>2</sup> Rive Droite Radiology Center, Geneva, Switzerland

<sup>3</sup> Division of Orthopaedics and Trauma Surgery, La Tour Hospital, Geneva, Switzerland

<sup>4</sup> Faculty of Medicine, University of Geneva, Geneva, Switzerland

**Abstract - Impingement and glenohumeral stability at critical tennis positions have never been dynamically evaluated. To this end, measuring the dynamic in-vivo shoulder kinematics is crucial. Motion capture using skin-mounted markers offers good solutions but none of the current techniques have reported translation values at the glenohumeral joint. The aims of this study were thus to develop a dedicated patient-specific measurement technique to accurately determine glenohumeral kinematics (rotations and translations), and to evaluate impingements and stability during dynamic movements in tennis players. Results showed that posterolateral impingements were frequent when serving.**

*Shoulder Kinematics, Tennis Players, Glenohumeral Instability, Glenohumeral Impingement*

## 1. INTRODUCTION

Shoulder pain and injury are common in tennis players. A majority of the shoulder pain is caused by impingement and instability due to repetitive lifting and overhead arm movements. During the late follow-through phase of forehand and the backhand preparation phase, subcoracoid impingement (contact between the coracoid process and the lesser tuberosity of the humeral head) [1] and anterosuperior impingement (contact between the reflection pulley and the anterosuperior glenoid rim) [2] could occur. During the late cocking stage of serve, subacromial impingement (contact between the anterior [3] or lateral acromion [4] and the superior humeral head) and posterolateral impingement [5] (contact between the greater tuberosity of the humeral head and the posterolateral aspect of the glenoid) could occur. The precise causes for these impingements remain unclear, but it is believed it could result from different factors (e.g., repetitive contact, glenohumeral instability, scapular orientation, etc.).

To our knowledge, impingement and glenohumeral instability at critical tennis positions have never been dynamically evaluated and are to date supposition. To achieve these goals, measuring the dynamic in-vivo shoulder kinematics is crucial, but remains a challenging problem due to its complicated anatomy and large range of motion (ROM). Unfortunately, the motion of the shoulder joints cannot be explored with standard Magnetic Resonance Imaging (MRI) or Computed Tomography (CT) because they are limited to static measurement and might therefore miss some specificities of dynamic motion. Fluoroscopy-based measurements provide sufficient accuracy for dynamic shoulder analysis, but they use ionizing radiation. Motion capture systems using skin-mounted markers are good solutions to non-invasively determine shoulder kinematics during dynamic movements. However, such systems are subject to soft tissue artifacts (STA). In the upper extremity, the scapula is particularly affected [6]. Moreover, none of the current motion capture techniques have reported translation values at the glenohumeral joint. This information is crucial to assess glenohumeral stability and to understand the mechanism of shoulder impingement.

The purpose of this study was to develop a dedicated patient-specific measurement technique based on optical motion capture and MRI to accurately determine glenohumeral kinematics (rotations and translations). The second objective was to evaluate impingements and stability during dynamic movements in tennis players.

## 2. MATERIAL AND METHODS

Ten intermediate or ex-professional tennis players (9♂, 1♀, mean age:  $39.7 \pm 8.9$  years) were recruited for this study. The dominant arm (right arm except for one participant) was used throughout testing. Ethical approval was gained from the local Institutional Review Board, and all participants gave their written informed consent.

### *MR imaging and bone models reconstruction*

All volunteers underwent a MR shoulder arthrography to prospectively assess all images for rotator cuff and labral or ligament lesions. MRI examinations were performed with a 1.5 T HDxT system (General Electric Healthcare, Milwaukee, USA). Based on the 3D MR images, patient-specific 3D models of the shoulder bones (humerus, scapula, clavicle and sternum) were reconstructed for each volunteer using ITK-SNAP software [7]. Local coordinate systems (Fig. 1a) were then established based on the definitions suggested by the International

Society of Biomechanics [8] to represent the thorax, clavicle, scapula and humerus segments using anatomical landmarks identified on the bone models and MR images. The glenohumeral joint center was calculated using a sphere fitting method [9].

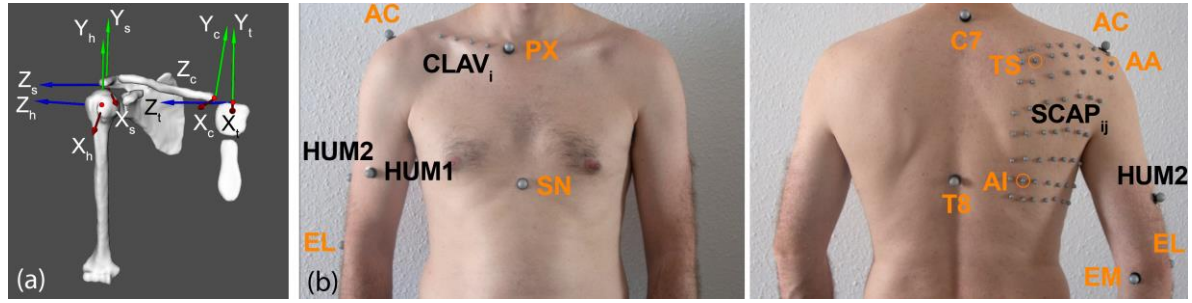


Figure 1. a) Bone coordinate systems for the thorax ( $X_t, Y_t, Z_t$ ), clavicle ( $X_c, Y_c, Z_c$ ), scapula ( $X_s, Y_s, Z_s$ ) and humerus ( $X_h, Y_h, Z_h$ ). b) Markers placement including markers placed on anatomical landmarks (orange) and technical markers (black). PX = xyphoid process, SN = sternal notch, AC = acromion, TS = trigonum spinae, AA = angulus acromialis, AI = angulus inferior, EL = lateral epicondyle, EM = medial epicondyle.

### Motion recording

Kinematic data was recorded using a Vicon MXT40S motion capture system (Vicon, Oxford Metrics, UK) consisting of 24 cameras sampling at 120 Hz. Participants were equipped with spherical retroreflective markers placed directly onto the skin (Fig. 1b). The setup included 4 markers ( $\varnothing$  14 mm) on the thorax, 4 markers ( $\varnothing$  6.5 mm) on the clavicle, 4 markers ( $\varnothing$  14 mm) on the upper arm and 57 markers (1x  $\varnothing$  14 mm on the acromion and a 7x8 grid of  $\varnothing$  6.5 mm) on the scapula. Additional markers were distributed over the body (non-dominant arm and legs) to confer a more complete visualization from general to detailed. Data from the subjects were acquired during tennis movements: forehand, backhand, flat and kick serves (3 trials each).

### Kinematic modeling

It was demonstrated that the use of global optimization could help reduce STA errors globally [10]. A kinematic chain consisting of four rigid bodies (thorax, clavicle, scapula and humerus) was thus developed using the subject's 3D bone models. The position and orientation of the thorax relative to the global coordinate system was defined with six degrees of freedom (DoF), and the sternoclavicular, acromioclavicular and glenohumeral joints were each defined as ball-and-socket joint (3 DoF) with loose constraints on the translations. Joint translations were thus permitted but limited. The optimal pose of the kinematic chain was obtained by finding the best transforms  $RT_s$  for every segment  $s$  that minimize the following equation:

$$\min \sum_{s=1}^4 \left( \sum_{i=1}^{n_s} \alpha_{si} \|RT_s x_{si} - y_{si}\|^2 \right) + \sum_{s=1}^3 \beta_s \|t_s\|^2 \quad (1)$$

This corresponds to the minimization of two terms: 1) the distances between the model-based ( $x_{si}$ ) and the measured ( $y_{si}$ ) marker coordinates in the segment's cluster ( $n_s$  markers in segment's cluster  $s$ ) with  $\alpha_{si}$  a weighting factor to reflect different degrees of STA, as described by [10]; 2) the translation penalty at each joint with  $\beta_s$  a weighting factor to control the amount of possible translation at the joint and  $t_s$  the relative translation of the segment  $s$  with respect to its proximal bone. For simplicity, equal weighting factors ( $\alpha_{si}$ ) were assigned to the markers of the thorax, clavicle and humerus clusters. Since STA is significantly lower at the flat portion of the acromion [6], markers of the scapular grid were given weight inversely proportional to their distance to the acromion. The weighting factors  $\beta_s$  were chosen to allow translation values of the same order of magnitude as translations reported in published data. To solve (1), we used a non-linear sequential quadratic programming algorithm [11]. Fig. 2 shows examples of computed tennis motion.

### Validation

A validation test involving six of the ten tennis players was performed. Kinematic data was collected simultaneously from an X-ray fluoroscopy unit (MultiDiagnost Eleva, Philips Medical Systems, The Netherlands) and the motion capture system during clinical motion patterns (flexion, abduction and internal-external rotation of the arm). Glenohumeral kinematics was derived from the marker position data and compared with the one obtained with the fluoroscopy gold-standard using a 3D-to-2D shape matching technique [12]. RMS errors for glenohumeral orientation were within  $4^\circ$  for each anatomical plane and between 1.9 and 3.3 mm for glenohumeral translations. Although the translation errors were significant, the results showed that the patterns of humeral translation computed with the model were in good agreement with previous works [12].

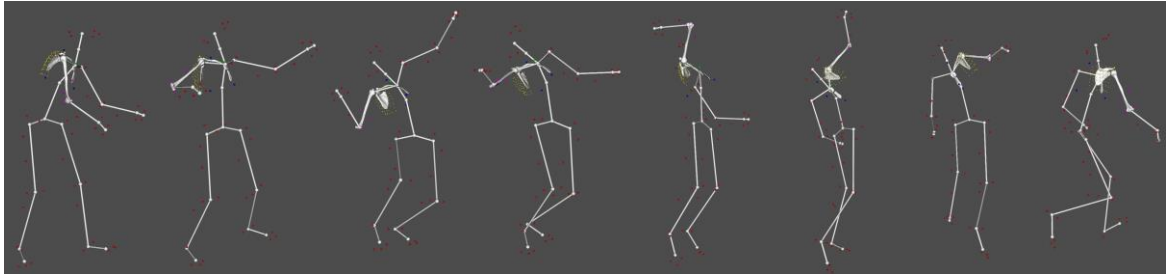


Figure 2. Kinematic animation of the shoulder (here the right shoulder joints) during flat serve, including a virtual skeleton used to better visualize and analyze the motion as a whole. Position 4, 7 and 8 are commonly known as the cocking, deceleration and finish stages, respectively.

### *Glenohumeral Stability and Impingement Analysis*

Glenohumeral stability was assessed during flat and kick serves at the late coking, deceleration and finish stages which are known to be the more demanding in terms of inertia and ROM. Glenohumeral translation was defined as the anterior-posterior and superior-inferior motion of the humeral head center relative to the glenoid coordinate system. This coordinate system was determined by an anterior-posterior X-axis and a superior-inferior Y-axis with origin placed at the intersection of the anterior-posterior aspects and superior-inferior aspects of the glenoid rim (Fig. 3a). Subluxation was defined as the ratio (in %) between the translation of the humeral head center and the radius of the width (anteroposterior subluxation) or height (superoinferior subluxation) of the glenoid surface. Instability was thus considered when the subluxation was  $> 50\%$ , which corresponds to a loss of congruence superior to half the radius of the width (or height) of the glenoid.

Impingements were evaluated at critical tennis positions (see Introduction). While visualizing the tennis player's shoulder joints in motion, minimum humero-acromial, humero-coracoid and humero-glenoid distances that are typically used for the diagnosis of impingements were measured (Fig. 3b). Given the thickness of the potential impinged tissues, impingement was considered when the computed distance was  $< 6$  mm for the humero-acromial distance and  $< 5$  mm for the other distances, as suggested in previous studies [13].

For all critical tennis positions, we calculated the frequency of impingement and the mean and standard deviations (SD) of the minimum humero-acromial, humero-coracoid and humero-glenoid distances. We also computed the percentage of subluxation at the different stages of serve.

### 3. RESULTS

No subcoracoid impingement was detected during the late follow-through phase of forehand and the backhand preparation phase, but anterosuperior impingements were observed in two subjects during forehand (Table 1). Anterior and lateral subacromial impingements occurred during the late cocking stage of serve in three and four subjects, respectively. Posterosuperior impingements during the late cocking stage of serve were the most frequent (7 subjects, 75%). In this position, glenohumeral translation was anterior (flat serve, mean: 34%; kick serve, mean: 34%) and superior (flat serve, mean: 12%; kick serve, mean: 13%). During the deceleration stage of serve, anterior and superior translation varied between 8-57% and between 5-34%, respectively. During the finish stage of serve, anterior translation was slightly more intense (flat serve, mean: 46%; kick serve, mean: 42%), while superior translation remained low (flat serve, mean: 3%; kick serve, mean: 0%). MR images revealed eleven rotator cuff lesions in five subjects, and six labral lesions in five subjects (two inferior, two posterior and two posterosuperior), which were relevant with respect to the detected impingements.

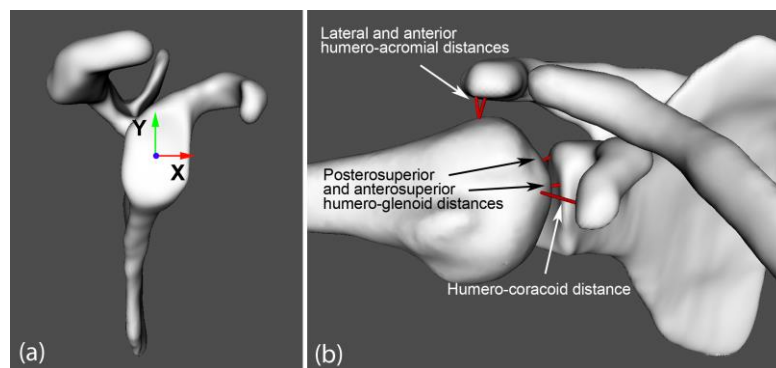


Figure 3. a) Definition of the glenoid coordinate system. b) Visualization of the humero-acromial, humero-coracoid and humero-glenoid distances during motion. The red lines represent the minimum distances.

Table 1. Frequency of impingement (%) and minimum humero-acromial, humero-coracoid and humero-glenoid distances (mean  $\pm$  SD) at critical tennis positions (n = 30; 10 subjects, 3 trials)

Distances [mm]	Flat serve	Kick serve	Forehand	Backhand
Humero-acromial (lateral)	29% 7.5 $\pm$ 3.2	42% 6.8 $\pm$ 3.7	-	-
Humero-acromial (anterior)	29% 7.4 $\pm$ 2.9	29% 7.0 $\pm$ 3.1	-	-
Humero-coracoid	-	-	0% 15.9 $\pm$ 1.6	0% 15.0 $\pm$ 2.7
Humero-glenoid (anterosuperior)	-	-	29% 5.5 $\pm$ 1.2	0% 6.9 $\pm$ 1.3
Humero-glenoid (posterosuperior)	76% 3.6 $\pm$ 1.4	75% 3.3 $\pm$ 1.8	-	-

#### 4. DISCUSSION

The kinematic data of this study was reconstructed using a kinematic chain model of the shoulder complex with loose constraints on joints translations. To our knowledge, this methodology is the first attempt to calculate both rotations and translations at the glenohumeral joint based on skin-mounted markers.

Thanks to this original and patient-specific measurement technique, shoulder impingement and stability were actively assessed and demonstrated in-vivo during tennis movements. Anterosuperior and subacromial impingements remained occasional in this population. No shoulder instability could be noted. However, posterosuperior impingement was frequent when serving. This shot seems thus to be the most harmful for the shoulder. Tennis players presented frequent radiographic signs of structural lesions which seem to be mainly related to posterosuperior impingement due to repetitive abnormal motion contacts [5]. This study is consistent with this hypothesis and offers novel insights into the analysis of shoulder impingement and instability that could, with future studies, be generalized to other shoulder pathologies and sports.

Future work will address the following points: the use of a biomechanical model of the glenohumeral joint taking into account the capsular ligaments to improve estimation of joint translations; the consideration in the simulation of the 3D shapes and motion of the cartilage, labrum and tendons to better assess impingement.

#### 5. ACKNOWLEDGMENT

This work was supported by grants from La Tour Hospital, Geneva, Switzerland, and from the European Society of Shoulder and Elbow Surgery.

#### 6. REFERENCES

- [1] Gerber, C., Terrier, F., Ganz, R., 1985. The role of the coracoid process in the chronic impingement syndrome. *JBJS Am* 67, 703-708.
- [2] Gerber, C., Sebesta, A., 2000. Impingement of the deep surface of the subscapularis tendon and the reflection pulley on the anterosuperior glenoid rim: a preliminary report. *J Shoulder Elbow Surg* 9, 483-490
- [3] Neer, C., 1972. Anterior acromioplasty for chronic impingement syndrome in the shoulder: a preliminary report. *JBJS Am* 54, 41-50.
- [4] Nyffeler, R.W., Werner, C.M.L., Sukthankar, A., Schmid, M.R., Gerber, C., 2006. Association of a large lateral extension of the acromion with rotator cuff tears. *JBJS Am* 88(4), 800-805.
- [5] Walch, G., Boileau, P., Noel, E., Donell, S., 1992. Impingement of the deep surface of the supraspinatus tendon on the posterior glenoid rim: an arthroscopic study. *J Shoulder Elbow Surg* 1, 238-245.
- [6] Warner, M., Chappell, P., Stokes, M., 2012. Measuring scapular kinematics during arm lowering using the acromion marker cluster. *Hum Mov Sci* 31, 386-396.
- [7] ITK-SNAP software, <http://www.itksnap.org/>
- [8] Wu, G., van der Helm, F., Veeger, H., Makhsouse, M., Roy, P. V., et al., 2005. ISB recommendation on definitions of joint coordinate systems of various joints for the reporting of human joint motion - part II: shoulder, elbow, wrist and hand. *J Biomech* 38, 981-992.
- [9] Schneider, P., Eberly, D., 2003. *Geometric Tools for Computer Graphics*. The Morgan Kaufmann Series in Computer Graphics and Geometric Modeling.
- [10] Lu, T., O'Connor, J., 1999. Bone position estimation from skin marker co-ordinates using global optimisation with joint constraints. *J Biomech* 32, 129-134.
- [11] Lawrence, C., Tits, A., 2001. A computationally efficient feasible sequential quadratic programming algorithm. *SIAM J Optim* 11(4), 1092-1118.
- [12] Matsuki, K., Matsuki, K., Yamaguchi, S., Ochiai, N., Sasho, T., et al., 2012. Dynamic in vivo glenohumeral kinematics during scapular plane abduction in healthy shoulders. *J Orthop Sports Phys Ther* 42(2), 96-104.
- [13] Chopp, J., Dickerson, C.R., 2012. Resolving the contributions of fatigue-induced migration and scapular reorientation on the subacromial space: An orthopaedic geometric simulation analysis, *Hum Mov Sci* 31, 448-460.